A COUPLED RESONANT FILTER BANK FOR THE SOUND SYNTHESIS OF NONLINEAR SOURCES

Samuel Poirot, Richard Kronland-Martinet, Stefan Bilbao

A COUPLED RESONANT FILTER BANK FOR THE SOUND SYNTHESIS OF NONLINEAR SOURCES

Samuel Poirot and Richard Kronland-Martinet

PRISM
Aix Marseille Univ, CNRS, PRISM
Marseille, France
poirot@prism.cnrs.fr

Stefan Bilbao

Acoustics and Audio Group
University of Edinburgh
Edinburgh, UK
s.bilbao@ed.ac.uk

ABSTRACT

This paper is concerned with the design of efficient and controllable filters for sound synthesis purposes, in the context of the generation of sounds radiated by nonlinear sources. These filters are coupled and generate tonal components in an interdependent way, and are intended to emulate realistic perceptually salient effects in musical instruments in an efficient manner. Control of energy transfer between the filters is realized by defining a matrix containing the coupling terms. The generation of prototypical sounds corresponding to nonlinear sources with the filter bank is presented. In particular, examples are proposed to generate sounds corresponding to impacts on thin structures and to the perturbation of the vibration of objects when it collides with an other object. The different sound examples presented in the paper and available for listening on the accompanying site tend to show that a simple control of the input parameters allows to generate sounds whose evocation is coherent, and that the addition of random processes allows to significantly improve the realism of the generated sounds.

1. INTRODUCTION

Modal synthesis operates according to the decomposition of the complex dynamic behavior of a vibrating object into contributions from modes, each oscillating independently at a single frequency. This approach, applicable to linear and time-invariant systems, is widely used and forms the basis for various physical modelling synthesis software packages [1] [2] and is closely related to sound synthesis methodologies employing filter banks [3] [4] [5].

For vibrating objects incorporating nonlinear effects, the modal interpretation must be generalized to include energy transfer between different modes (among other things such as e.g. frequency shifting of modes over time). It may cause the delayed and sustained appearance of tonal components that cannot be generated by linear filtering. This complex phenomenon, widely studied for the typical case of thin plates and shells [6] [7], can be modelled and solved under certain conditions. The numerical solution of the Föppl-von Kármán system [8, 9] that governs the underlying dynamics of nonlinear thin plates at moderate vibration amplitudes yields realistic and convincing sound synthesis [10], but at heavy computational cost. Ducceschi and Touzé [11] propose the modal resolution of the system with the offline calculation of coupling coefficients. They manage under certain approximations to significantly reduce the computation time without being able to achieve real-time sound synthesis (about 8 times real-time on a CPU) [12]. Another typical case of coupling between modes induced by nonlinear phenomena concerns collisions in musical instruments [13] and has been the subject of various studies, including on modal interactions [14]. Computational cost for synthesis can also be heavy in such cases.

For synthesis purposes, and particularly if real-time performance is the ultimate aim, it can be useful to depart from strict physical models, and examine modal interactions from a perceptual point of view. Skare and Abel [15] perform real-time modal synthesis of crash cymbals with a GPU-accelerated modal filterbank. Their method consists in identifying the modal parameters (including a rough approximation of the couplings) on recorded sounds, although the energy transfer mechanism is unspecified.

In this paper, we design coupled filters based on the design proposed by Mathews and Smith [16] and adapted by Skare and Abel [15] to incorporate energy transfer. In particular, we propose an equivalence between the power of the signal corresponding to a tonal component and the energy of a vibration mode from an equivalent physical system to ensure energy conservation during transfers. Inter-modal energy transfer is encoded in a matrix containing all the coupling coefficients. The aim of this paper is not to propose a synthesis model performing an accurate simulation of a physical system. Instead, we seek to develop a framework allowing direct modelling of sounds targeted to the way they are perceived. This results in an efficient way to generate sounds evoking nonlinear sources and can yield real-time event-driven synthesis of sounds in virtual or augmented reality environments, a particularly active field of research [17] [18].

Some background on modal synthesis and linear filtering is given in Section 2. Then, the coupling between the filters is presented in Sec.3, the stability of the filters is discussed in Sec.3.2, and the definition of the matrix containing the coupling terms is proposed in Sec.4. Various example systems used to generate prototypical sounds are presented in Sec.5. Sound examples are available online at the following address [19].

2. MODAL SYNTHESIS AND LINEAR FILTERING

The modal resolution of a linear partial differential equations (PDE) system describing the vibrations of a resonant object is well-described in various texts [20]. Solutions are of the following form for the displacement w depending on a spatial coordinate $\mathbf{r}$ and time t:

$$w(\mathbf{r},t) = \underbrace{w_h(\mathbf{r},t)}_{\text{homogeneous solution}} + \underbrace{w_p(\mathbf{r},t)}_{\text{particular solution}}, \quad (1)$$

where

$$w_h(\mathbf{r},t) = \sum_{i=1}^{\infty} e^{-\alpha_i t}\left[A_i\cos(\omega_i t+\varphi_i)\right]\phi_i(\mathbf{r}) \quad (2a)$$

$$w_p(\mathbf{r},t) = \sum_{i=1}^{\infty} \left(g_i(t) * h_i(t)\right)\phi_i(\mathbf{r}), \quad (2b)$$

Here, $*$ represents a convolution operation, and the impulse response $h_i(t)$ of the following form:

$$h_i(t) = \frac{1}{\omega_i} e^{-\alpha_i t}\sin(\omega_i t) \quad (3)$$

the function $\phi_i(\mathbf{r})$ is the i^{th} mode's shape or basis function, ω_i and α_i are the angular frequency and the damping coefficient of the i^{th} mode, respectively. The constants A_i and φ_i derive from the initial conditions and $g_i(t)$ is the modal excitation (projection of an excitation source $g(\mathbf{r},t)$ onto the modal basis functions).

One may note that the modal model does not necessarily derive from the solution of partial differential equations. The modal parameters may be identified directly from experimental measurements (recording) or from numerical simulations.

A straightforward approach to numerical solution at a sample rate f_s in Hz is to use recursive filters with an exponentially-damped sinusoidal impulse response (IIR). The filter proposed by Mathews and Smith [16] has this property. The implementation of this filter consists in calculating, for each time step n, the imaginary part of a complex number $z(n)$ whose rotation speed in the complex plane is constant and corresponds to the angular frequency ω of the exponentially damped sinusoid:

$$y(n) = \mathrm{Im}(z(n)) \qquad \text{where} \qquad z(n+1) = Zz(n)+u(n) \quad (4)$$

with $u(n)$ the source of the filter, and Z the constant modification of the phase and modulus in one time step:

$$Z = e^{-\alpha/f_s}e^{j\omega/f_s} = X + jY \quad (5)$$

with $X = e^{-\alpha/f_s}\cos(\omega/f_s)$ and $Y = e^{-\alpha/f_s}\sin(\omega/f_s)$.

The recurrence equation on the complex sequence $z(n)$ is computed by the following system including a recurrence equation for the real part $x(n) = \mathrm{Re}(z(n))$ and a recurrence equation for the imaginary part $y(n) = \mathrm{Im}(z(n))$, which is the output of the filter:

$$\begin{aligned} x(n+1) &= \mathrm{Re}(z(n+1)) = Xx(n) - Yy(n) + u(n) \\ y(n+1) &= \mathrm{Im}(z(n+1)) = Yx(n) + Xy(n) \end{aligned} \quad (6)$$

for a real source $u(n) \in \mathbb{R}$.

3. COUPLING BETWEEN THE FILTERS

3.1. Principle and implementation

Consider N filters defined as in the previous section in parallel and we wish to couple them. We note $z_i(n)$ the complex sequence corresponding to the i^{th} filter, with $x_i(n)$ its real part and $y_i(n)$ its imaginary part (corresponding to the output signal of the filter). The source for the i^{th} filter, corresponding to the projection of the source of the filter bank $u(n)$ onto the i^{th} modal basis function, is noted $u_i(n)$.

The mechanical energy corresponding to the vibration of a mode is proportional to the square of the amplitude of the displacement. From a signal point of view, the square of the amplitude of a tonal component corresponds to twice the power of the signal. Postulating a linear relation between the displacement of the structure and the sound produced, we have chosen to model the energy transfers between the modes by power transfers between the filters [21]. If we only look at the power evolutions linked to the energy transfers (by postulating a null source), we write the following recurrence relation on the powers of the output signals of the different filters P_i:

$$P_i(n+1) = \left(P_i(n) + \underbrace{T_i(n)}_{\text{transfer}}\right)\underbrace{e^{-2\alpha_i/f_s}}_{\text{losses}} \quad (7)$$

with

$$P_i(n+1) \geq 0 \Leftrightarrow P_i(n) + T_i(n) \geq 0, \quad (8)$$

and $P_i(n)$ the power of the tonal component:

$$P_i(n) = \frac{|z_i(n)|^2}{2} = \frac{1}{2}(x_i(n)^2 + y_i(n)^2) \quad (9)$$

$x_i(n), y_i(n) \in \mathbb{R}$.

Thus, we can express the variation of the modulus of $z_i(n)$ due to energy transfer between two time steps:

$$|z_i(n+1)| = \sqrt{|z_i(n)|^2 + 2T_i(n)}\, e^{-\alpha_i/f_e} \quad (10)$$

We can define an amplitude ratio between the modulus for two consecutive time steps if $|z_i(n)| \neq 0$:

$$\frac{|z_i(n+1)|}{|z_i(n)|} = \underbrace{\sqrt{1 + \frac{2T_i(n)}{|z_i(n)|^2}}}_{\text{transfer}}\ \underbrace{e^{-\alpha_i/f_e}}_{\text{losses}} \quad (11)$$

Thus, we can modify the recurrence equation defined in the previous section (see Eq.(4)) by incorporating the modulus variations due to energy transfers. It gives the following recurrence relation for z_i, including the source and phase variations:

$$z_i(n+1) = \begin{cases} \sqrt{2T_i(n)}Z_i + u_i(n) & \text{if } z_i(n) = 0 \\ \sqrt{1 + \frac{2T_i(n)}{|z_i(n)|^2}}Z_i z_i(n) + u_i(n) & \text{else} \end{cases} \quad (12)$$

with $Z_i = e^{-\alpha_i/f_s}e^{j\omega_i/f_s} = X_i + jY_i$, as defined in Eq(5). One can note that $T_i(n) > 0$ if $z_i(n) = 0$ (see Eq.(8)). This implies that the term $\sqrt{2T_i(n)}$ is real in the first part of Eq.(12).

Finally, we can write the system of equations for the implementation of the filters (see Figure 1 for a representation in block diagram):

$$\begin{aligned} x_i(n+1) &= \mathrm{Re}(z_i(n+1)) = X_i\tilde{x}_i(n) - Y_i\tilde{y}_i(n) + u_i(n) \\ y_i(n+1) &= \mathrm{Im}(z_i(n+1)) = Y_i\tilde{x}_i(n) + X_i\tilde{y}_i(n) \end{aligned} \quad (13)$$

with

$$\tilde{x}_i(n) = \begin{cases} \sqrt{2T_i(n)} & \text{if } z_i(n) = 0 \\ \sqrt{1 + \frac{2T_i(n)}{|z_i(n)|^2}}\, x_i(n) & \text{else} \end{cases}$$

$$\tilde{y}_i(n) = \begin{cases} 0 & \text{if } z_i(n) = 0 \\ \sqrt{1 + \frac{2T_i(n)}{|z_i(n)|^2}}\, y_i(n) & \text{else} \end{cases} \quad (14)$$

In this way, power can be transferred among the different filters without affecting the phases. The coupling intervenes in the calculation of the transfer terms $T_i(n)$ which ultimately involve the other filters (see Figures 1 and 2).

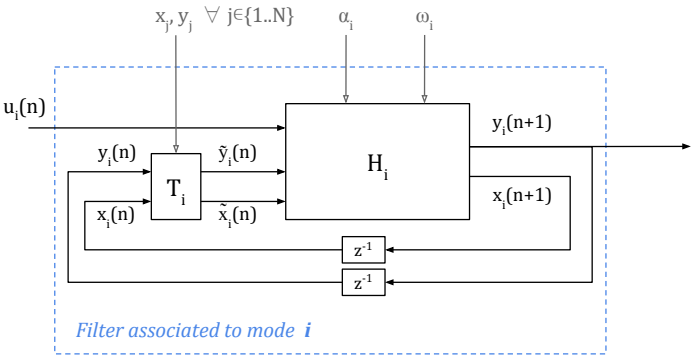

Figure 1: *Block diagram of a filter for the generation of the signal corresponding to a vibration mode. u corresponds to the source entering this particular filter and the block T_i corresponds to the calculation involving the states of other filters (coupling term).*

3.2. Energy and stability

A sufficient condition for the stability of the filter bank is to impose a non-positivity constraint for the transfer terms:

$$\sum_{i=1}^{N} T_i(n) \leq 0 \tag{15}$$

This condition impedes the creation of energy during transfer between modes for an equivalent physical system.

Also, the sum is bounded by the condition defined in Eq.(8) (a filter cannot transfer more power than it possesses):

$$\sum_{i=1}^{N} T_i(n) \geq -\sum_{i=1}^{N} P_i(n) \tag{16}$$

One can note that it is possible to consider a less restrictive stability condition that binds the transfer term to be lower than the power decrease due to losses:

$$\begin{aligned} &\sum_{i=1}^{N} \left(P_i(n) + T_i(n)\right)\, e^{-2\alpha_i/f_s} \leq \sum_{i=1}^{N} P_i(n) \\ &\quad \Leftrightarrow \quad \sum_{i=1}^{N} T_i(n)\, e^{-2\alpha_i/f_s} \leq \sum_{i=1}^{N} P_i(n) \left(1 - e^{-2\alpha_i/f_s}\right) \end{aligned} \tag{17}$$

However, this condition cancels the effect of dissipation and is not consistent with an equivalent physical system. We prefer to consider the condition presented Eq.(15) for the rest of the document.

4. DISTRIBUTION MATRIX

This section presents a formalism for the calculation and control of the coupling between filters. The challenge is to arrive at a model simple enough to be controllable (i.e., to be able to predict the sound outcome of a manipulation of the parameters) and complete enough to allow the matching of modal trajectories to a range of nonlinear phenomena.

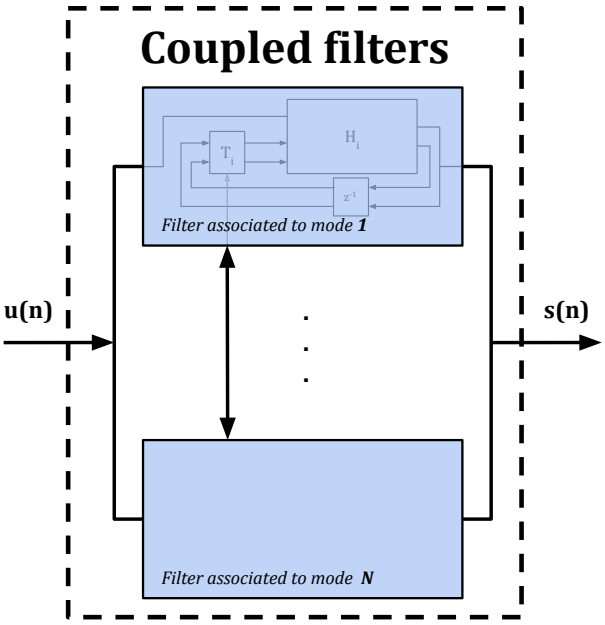

Figure 2: *Schematic representation of the coupled filter bank. the double arrow connecting the two boxes represents the coupling between the filters through the transfer vector* $\mathbf{t}$*. The output of the filter bank is the sum of the outputs of the filters* $s(n) = \sum_{i=1}^{N} y_i(n)$

Now define the column vectors $\mathbf{p}(n) = [P_1(n), \ldots, P_N(n)]^T$ and $\mathbf{t}(n) = [T_1(n), \ldots, T_N(n)]^T$. The power transfers between the tonal components $\mathbf{t}(n)$ at a given time step n are defined as:

$$\mathbf{t}(n) = \mathbf{M}\left[\mathbf{p}(n) - \boldsymbol{\tau}\right]_+ . \tag{18}$$

Here, $[\cdot]_+$ indicates the "positive part of", i.e., $[\zeta]_+ = \frac{1}{2}(\zeta + |\zeta|)$. An $N \times 1$ column vector $\boldsymbol{\tau}$ containing the thresholds τ_i, $i = 1, \ldots, N$ at which transfers are activated for each tonal component has also been introduced here.

Thus, the calculation of the transfer terms is performed by the matrix product of an $N \times N$ redistribution matrix $\mathbf{M}$ with the vector resulting from the positive part of the difference between the power of each frequency component $\mathbf{p}(n)$ and the associated threshold $\boldsymbol{\tau}$. In other words, the transfer terms $T_i(n)$ are proportional to the excess power above the corresponding threshold and the terms of the matrix $\mathbf{M}$ define the proportions distributed and received by each other component. Note that this relation is not an immediate consequence of a physical model but is a heuristic means of capturing salient phenoemna in a physical system. Our focus is on the design of a synthesis process with a predictable sound outcome rather than on the simulation of a physical system.

To respect the stability condition Eq.(15), we set the sum of all values of a given column of the matrix $\mathbf{M}$ to be lower or equal to zero. If M_{ij} is the i,jth entry of $\mathbf{M}$, then

$$\sum_{i=1}^{N} M_{ij} \leq 0 \;\; \forall\, j \;\; \Rightarrow \;\; \sum_{i=1}^{N} T_i(n) \leq 0 \tag{19}$$

The diagonal entries M_{jj} of the matrix $\mathbf{M}$ define the proportion of power of the jth mode that will be redistributed to other modes and the other terms of the column M_{ij} define the quantity that the ith mode will receive from this redistribution.

An efficient way to define the coefficients of the matrix is to use the following expression:

$$M_{ij} = \eta\lambda \frac{a_{ij}}{\sum_{i=1}^{N} a_{ij}} - \lambda\delta_{ij} \tag{20}$$

Where a_{ij} is a coefficient weighting the redistribution from the jth mode to the ith mode. In this formulation, the stability of the filter bank is ensured for arbitrary a_{ij}, provided that at least one value per column is non-zero and that $0 \leq \eta \leq 1$. η corresponds to the efficiency of the transfers ($\eta = 1 \Rightarrow \sum T_i(n) = 0$). λ is the proportion of power above threshold transferred to other modes at each time step ($0 \leq \lambda \leq 1$). The values of the off-diagonal elements M_{ij} of the matrix $\mathbf{M}$ are the proportion of energy transferred by the mode j that will be received by the mode i.

The i^{th} transfer term $T_i(n)$ can be expressed as follows:

$$T_i(n) = \underbrace{\eta\lambda \sum_{j=1}^{N} \left[\frac{a_{ij}}{\sum_{i=1}^{N} a_{ij}} \left(P_j(n) - \tau_j\right) \right]}_{\text{positive contribution } T_{i+}(n)} - \underbrace{\lambda \left(P_i(n) - \tau_i\right)}_{\text{negative contribution } T_{i-}(n)} \tag{21}$$

5. EXAMPLES

Nonlinear vibration leads to complex phenomena that can produce subtle and chaotic variations in radiated sound. We can reduce the complexity of the model and propose a heuristic that attempts to maintain the essential perceptual attributes of an object vibrating under nonlinear conditions. The resulting synthetic sound is nevertheless less realistic and versatile than sounds generated by the direct resolution of physical models (such as, e.g., the Föppl-von Kármán system) although the synthesis quality can be improved by using random processes in the implementation of the algorithms.

The coupled filter bank proposed here is dependent on many parameters: the number of filters N, the oscillation frequencies ω_i and damping α_i for each filter, the coefficients a_{ij} and the parameters λ and η for the definition of the redistribution matrix $\mathbf{M}$, and the thresholds τ_i. Strategies for setting these parameters are presented in two cases of musical interest. In the case of nonlinear plate vibration, energy is transferred to filters of near frequency in order to generate a gradual cascade of energy towards the high-frequency range. In the case of a string colliding with a rigid object, in contrast, there is simultaneous transfer or energy to many frequency components.

5.1. Energy cascade in thin plates

Consider a thin rectangular plate (according to the Kirchhoff model [22]), with mass density ρ kg$\cdot$ m^{-3}, thickness H m, and flexural rigidity D in kg$\cdot$m$^2\cdot$s^{-2}, and side lengths L_x and L_y in m. If the plate is simply supported on all its edges, the modal frequencies ω_{lm} and modal shapes $\phi_{lm}(x, y)$ can be expressed as follows [23]:

$$\omega_{lm} = \frac{\pi^2}{L_x^2}\sqrt{\frac{D}{\rho H}}\left(l^2 + \nu^2 m^2\right) \quad \phi_{lm}(x, y) = \sin(l\pi x)\sin(m\pi y) \tag{22}$$

Here, $\nu = L_x/L_y$ is the plate aspect ratio, or the ratio between the length and width of the plate. The integer indices $l, m \geq 1$ correspond to the number of vibration nodes in the main directions of the rectangular plate (Cartesian coordinates (x, y)) with x and y being normalized by the length of the plate in the corresponding direction (so that $0 \leq x, y \leq 1$).

For a point excitation force located at (x_e, y_e), we can compute the modal forces using the mode shapes evaluated at the excitation point as $\phi_{lm}(x_e, y_e)$. We define the source of the l, mth filter as follows:

$$u_{lm}(n) = \sin(l\pi x_e)\sin(m\pi y_e)u(n) \tag{23}$$

where $u(n)$ is the global excitation function.

We use a raised sinusoid for the excitation force (as proposed in [4] and [24]) to simulate an impact:

$$u(n) = \begin{cases} A\sin^2(\pi n/N_{ex}) & \text{if } n \leq N_{ex} \\ 0 & \text{else} \end{cases} \tag{24}$$

For typical plate strikes, the strike duration N_{ex}/f_s in seconds is on the order of 1-4 ms.

The damping coefficients are chosen according to an exponential law, as proposed by Aramaki et al.[25], with parameters that are set to evoke a metallic object:

$$\alpha_{lm} = e^{(\alpha_G + \omega_{lm}\alpha_R)} \tag{25}$$

with $\alpha_R = 4 \times 10^{-5}$ and $\alpha_G = 0.33220$. This set of parameters permits direct modal synthesis for linear plate vibration. To each pair of indices (l, m) we associate an index i (perhaps chosen in terms of increasing modal frequency) corresponding to the filter number used to generate the corresponding tonal component.

In order to produce the cascade of energy towards the high frequency components, we carry out transfers between filters whose frequencies are close. Indeed, the energy supplied by the impact is localised at low frequencies and transfers directed towards the neighbouring modes allow the progressive appearance of higher frequency components. The weighting coefficients a_{ij} can be set as follows (see Figure 3):

$$a_{ij} = \left[1 - \frac{|f_j - f_i|}{\Delta f}\right]_+ \tag{26}$$

with $f_i = \frac{\omega_i}{2\pi}$

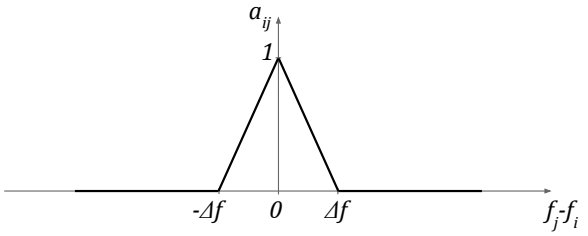

Figure 3: *Value of the coefficient a_{ij} as a function of the frequency difference between filter i and j.*

We set $\eta = 1$ (ensuring conservation of energy during the redistribution). The cascade can be mainly controlled by λ, or by the definition of thresholds τ_i (see Figures 4 and 5).

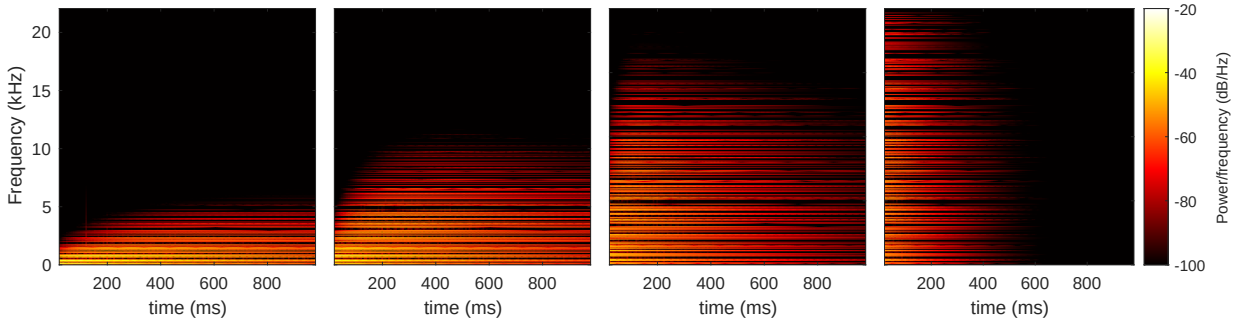

Figure 4: *Spectrograms of output for filters whose frequency corresponds to the modal frequency of a thin plate for different values of λ ($\tau_i = 0$). From left to right: $\lambda = 0.001$, $\lambda = 0.01$, $\lambda = 0.1$, $\lambda = 1$. We can observe that the energy cascade spreads faster and higher in frequency with the increase of λ. Transfers are performed at each time step.*

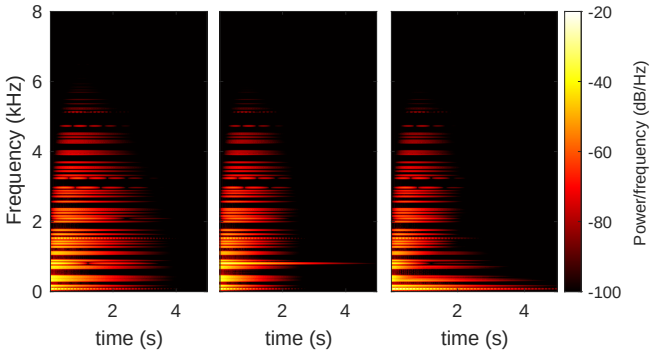

Figure 5: *Spectrograms of output for filters whose frequency corresponds to the modal frequency of a thin plate for different thresholds τ_i. Left: $\tau_i = 0$; middle: $\tau_i = 0$ except for $i = 10$ where $\tau_1 0 = 1$; right: τ_i is half the excitation amplitude. All tonal components decay simultaneously when the thresholds are zero (left). A component emerges and decays more slowly when its threshold is non-zero (middle). When all thresholds are different from zero, we observe a usual exponential decay after the delayed appearance of the high frequency component (right).*

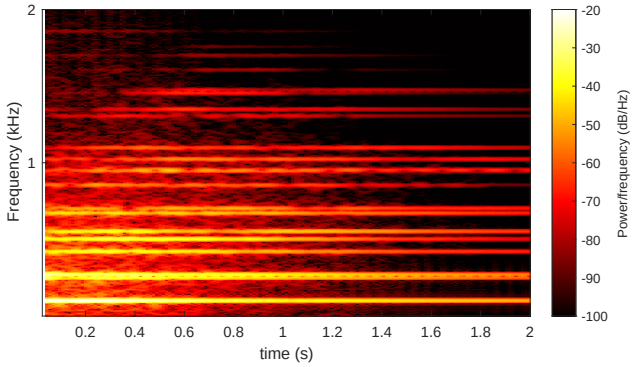

Figure 6: *Spectrogram of output for filters whose frequency corresponds to the modal frequency of a thin plate. The random modulation of the redistributions induces rapid variations in the amplitude of the tonal components which generate noise and beating in the signal.*

In the case of wave turbulence in plates [26], couplings between modes can lead to rapid variations in amplitude and frequency leading to a chaotic regime. In the chaotic regime, the resulting signal is noisy, and difficult to reproduce by a set of tonal components. One way to reproduce this phenomenon with the coupled filters presented in this paper is to pass randomized phases to the positive contributions of the transfer term in the source. In this way, the tonal components are subject to rapid random amplitude modulations that can evoke the chaotic phenomenon occurring during wave turbulence in the plates (see Figure 6).

5.2. Collisions in sound production

The perturbation of the vibrations of an object when colliding with an obstacle can lead to different types of sound events. In the typical case of a guitar, the player can choke the string, mute it, play a natural harmonic. The string can also interact with the soundboard (slap, string buzz).

The model of a vibrating string with simply supported boundary conditions gives the following modal frequencies and shapes:

$$\omega_i = i\omega_1 \qquad \phi_i(x) = \sin(i\pi x) \tag{27}$$

where here, the spatial coordinate x is normalized by the length of the string ($0 \leq x \leq 1$). For a point excitation force located at x_e, the source of the i^{th} filter can be defined as:

$$u_i(n) = \sin(i\pi x_e)u(n) \tag{28}$$

We use the same excitation force and damping model than previously (see Eqs.(24) and (25)).

The evocation of an obstacle disturbing the vibrations of the string requires the definition of thresholds that correspond to the location of the obstacle. We propose thresholds corresponding to the maximum amplitude of modal displacements without colliding with a virtual obstacle positioned at x_c, y_c, where y_c is the vertical displacement of the obstacle relative to the string:

$$\tau_i = \frac{1}{2}\left(\frac{y_c}{\sin(i\pi x_c)}\right)^2 \tag{29}$$

We define a redistribution matrix with all columns being identical in order to cause a simultaneous redistribution to a set of tonal components. The coefficients a_{ij} are defined as follows:

$$a_{ij} = |\sin(i\pi x_c)|\xi_i(f_i) \tag{30}$$

with $\xi_i(f_i)$ a parameter depending on the frequency allowing weighting of the redistribution according to the filter frequency. We define $\xi_i(f_i)$ as the Fourier transform of the raised cosine, an approximation of the force profile caused by a collision (as defined for the source, Eq.(24)):

$$\xi_i = \text{sinc}(f_i\gamma) + \frac{1}{2}\left(\text{sinc}(f_i\gamma - 1) + \text{sinc}(f_i\gamma + 1)\right) \tag{31}$$

with f_i the frequency of the i^{th} filter and γ a parameter corresponding to the duration of the raised cosine. This results in a cut-

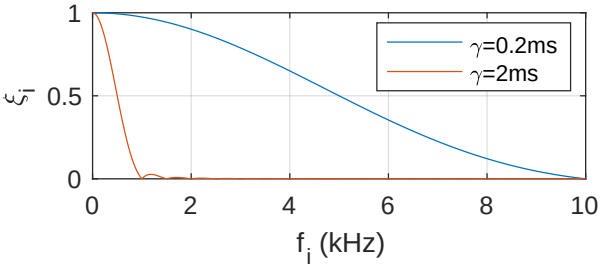

Figure 7: *Value of ξ_i as a function of the frequency of filter i.*

off frequency beyond which there is no more transfer (see Figure 7). Various examples of sound outputs for different configurations are presented—see Figures 8 and 9.

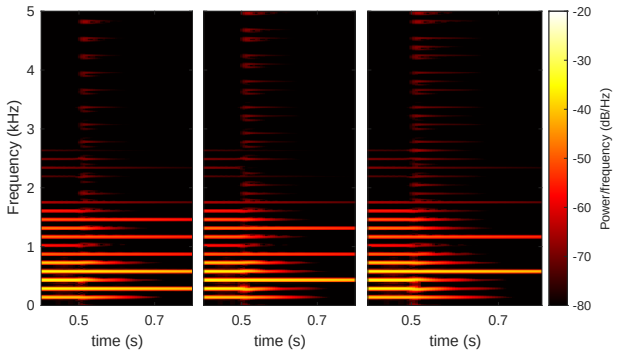

Figure 8: *Spectrograms of output for filters whose frequency are harmonic for different values of x_c ($y_c = 0$, $\gamma = 2 \times 10^{-4}s$, $\lambda = 0.25$, $\nu = 0.5$). Transfers are performed every 294 samples for times greater than 500ms, which corresponds to a collision every 6.67ms (150Hz). From left to right: $x_c = 1/2$, $x_c = 1/3$, $x_c = L/4$. We can observe that the transfer does not affect even harmonics (resp. multiples of 3 and 4) for $x_c = 1/2$ (resp.$x_c = 1/3$ and $x_c = L/4$), which allows the reproduction of a natural harmonic played on a guitar.*

Collisions in musical instruments may be the source of more subtle phenomena than a simultaneous appearance of various frequency components. The cases of string buzz and tanpura can be

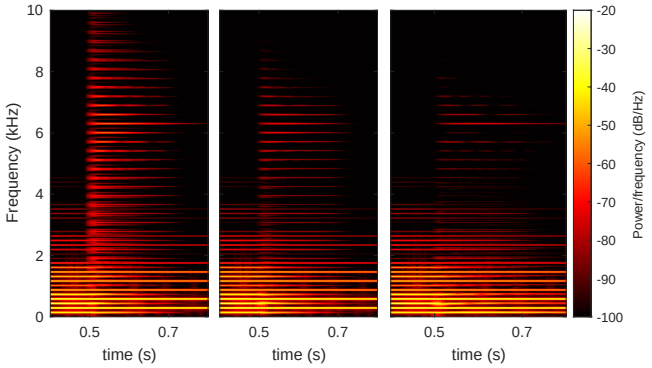

Figure 9: *Spectrograms of output for filters whose frequency are harmonic for different values of ν and γ ($x_c = 1/2$, $y_c = 0$). From left to right: ($\nu = 0.5$, $\gamma = 2 \times 10^{-4}s$), ($\nu = 0.15$, $\gamma = 2 \times 10^{-4}s$), ($\nu = 0.5$, $\gamma = 2 \times 10^{-3}s$). Transfers are performed every 294 samples for times greater than 500ms, which corresponds to a collision every 6.67ms (150Hz). There is a lower increase in the high-frequency components and a faster dissipation of all the tonal components involved in the redistribution as the efficiency decreases. As γ increases, there is also less energy distributed to the high-frequency components, but this energy is not dissipated and remains in the low-frequency components.*

approached by introducing random processes into the redistribution, as has been done for chaotic phenomena in plates (see Figure 10).

It is possible to apply the same principle for the generation of sounds corresponding to collisions with 2D objects. For example, we can generate muted plate sounds (see Figure 11).

6. CONCLUSION AND FURTHER WORK

In this paper, we have presented the design of coupled resonant filters geared towards the emulation of mode coupling effects in nonlinear vibrating structures. This filter bank allows efficient and real-time sound synthesis even for a large number of filters. The coupling, performed without modifying the phase, introduces predictable and controllable effects on the output signal. The terms controlling the coupling between the different filters are grouped in a matrix whose definition is the main challenge. The setting of the parameters of the sound synthesis process is presented through various examples corresponding to sources whose behavior is nonlinear. A simple setting allows the generation of typical sounds, though sometimes with an unnatural character. The introduction of random processes in the energy redistribution can add a lot in terms of plausibility.

Future work will be concerned with determining which sound morphologies are important from a perceptual point of view for the recognition of sound events [27] corresponding to nonlinear phenomena in order to reproduce them with this coupled filter bank. This could lead to the development of environmental sound synthesizers and virtual musical instruments (e.g. tanpura, cymbal ...), or to non-linear audio effects (such as the nonlinear reverberation of a snare drum due to the wires held under tension against the lower drumskin). The filter bank presented in this paper can also be used as an abstract sound creation tool. In this context, the chal-

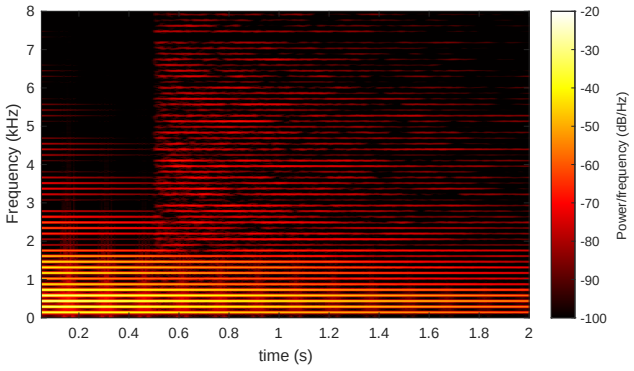

Figure 10: *Spectrograms of output for filters whose frequency are harmonic with the introduction of random processes during the redistribution ($\lambda = 0.001$, $\nu = 0.9$, $x_c = 0.38$, $y_c = 0.001$, $\gamma = 2 \times 10^{-4}s$). Transfers are performed every 294 samples for times greater than 500ms, which corresponds to a collision every 6.67ms (150Hz).*

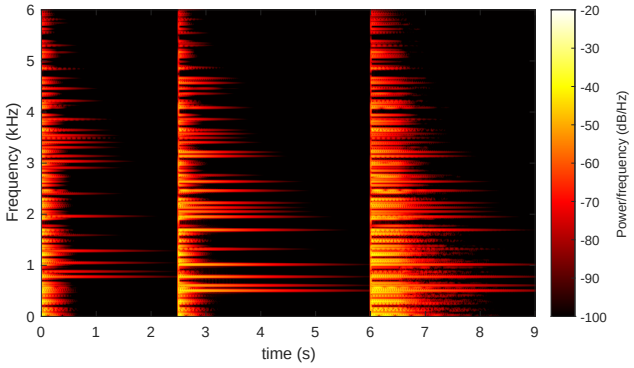

Figure 11: *Spectrograms of output for filters whose frequency corresponds to the modal frequency of a thin plate. here $\nu = 0$ and we observe the quick dissipation of certain tonal components for three distinct impacts, which creates a sensation of choking.*

lenge would be to design intuitive control for use in a musical or sound design context.

7. REFERENCES

[1] Jean-Marie Adrien, "The missing link: Modal synthesis," in *Representations of musical signals*, pp. 269–298. 1991.

[2] Joseph Derek Morrison and Jean-Marie Adrien, "Mosaic: A framework for modal synthesis," *Computer Music Journal*, vol. 17, no. 1, pp. 45–56, 1993.

[3] Davide Rocchesso, "The ball within the box: a sound-processing metaphor," *Computer Music Journal*, vol. 19, no. 4, pp. 47–57, 1995.

[4] Kees Van Den Doel, Paul G Kry, and Dinesh K Pai, "Foleyautomatic: physically-based sound effects for interactive simulation and animation," in *Proceedings of the 28th annual conference on Computer graphics and interactive techniques*, 2001, pp. 537–544.

[5] Simon Conan, Etienne Thoret, Mitsuko Aramaki, Olivier Derrien, Charles Gondre, Sølvi Ystad, and Richard Kronland-Martinet, "An intuitive synthesizer of continuous-interaction sounds: Rubbing, scratching, and rolling," *Computer Music Journal*, vol. 38, no. 4, pp. 24–37, 2014.

[6] KA Legge and Neville H Fletcher, "Nonlinearity, chaos, and the sound of shallow gongs," *The Journal of the Acoustical Society of America*, vol. 86, no. 6, pp. 2439–2443, 1989.

[7] Antoine Chaigne, Cyril Touzé, and Olivier Thomas, "Nonlinear vibrations and chaos in gongs and cymbals," *Acoustical science and technology*, vol. 26, no. 5, pp. 403–409, 2005.

[8] A. Föppl, *Vorlesungen über technische Mechanik*, Druck und Verlag von B.G. Teubner, Leipzig, 1907.

[9] T. von Kármán, "Festigkeitsprobleme im maschinenbau," *Encyklopädie der Mathematischen Wissenschaften*, vol. 4, no. 4, pp. 311–385, 1910.

[10] Stefan Bilbao, "A family of conservative finite difference schemes for the dynamical von karman plate equations," *Num. Meth. PDE*, vol. 24, no. 1, pp. 193–216, 2008.

[11] Michele Ducceschi and Cyril Touzé, "Modal approach for nonlinear vibrations of damped impacted plates: Application to sound synthesis of gongs and cymbals," *Journal of Sound and Vibration*, vol. 344, pp. 313–331, 2015.

[12] Michele Ducceschi and Cyril Touzé, "Simulations of nonlinear plate dynamics: an accurate and efficient modal algorithm," in *18th International Conference on Digital Audio Effects (DAFx-15)*, 2015.

[13] Stefan Bilbao, Alberto Torin, and Vasileios Chatziioannou, "Numerical modeling of collisions in musical instruments," *Acta Acustica united with Acustica*, vol. 101, no. 1, pp. 155–173, 2015.

[14] Clara Issanchou, Stefan Bilbao, Jean-Loic Le Carrou, Cyril Touzé, and Olivier Doaré, "A modal-based approach to the nonlinear vibration of strings against a unilateral obstacle: Simulations and experiments in the pointwise case," *Journal of Sound and Vibration*, vol. 393, pp. 229–251, 2017.

[15] Travis Skare and Jonathan Abel, "Real-time modal synthesis of crash cymbals with nonlinear approximations, using a gpu," in *Proc. 22nd Int. Conf. Dig. Audio Effects*, 2019.

[16] Max Mathews and Julius O Smith, "Methods for synthesizing very high q parametrically well behaved two pole filters," in *Proceedings of the Stockholm Musical Acoustics Conference (SMAC 2003)(Stockholm), Royal Swedish Academy of Music (August 2003)*, 2003.

[17] Laurent Pruvost, Bertrand Scherrer, Mitsuko Aramaki, Sølvi Ystad, and Richard Kronland-Martinet, "Perception-based interactive sound synthesis of morphing solids' interactions," in *SIGGRAPH Asia 2015 Technical Briefs*, pp. 1–4. 2015.

[18] Chuang Gan, Jeremy Schwartz, Seth Alter, Damian Mrowca, Martin Schrimpf, James Traer, Julian De Freitas, Jonas Kubilius, Abhishek Bhandwaldar, Nick Haber, et al., "Threedworld: A platform for interactive multi-modal physical simulation," *arXiv preprint arXiv:2007.04954*, 2020.

[19] S. Poirot, "Sound examples," Available at https://www.prism.cnrs.fr/publications-media/DaFXPoirot/, accessed April 07, 2023.

[20] Zhi-Fang Fu and Jimin He, *Modal analysis*, Elsevier, 2001.

[21] S. Poirot, *Des non-linéarités physiques à la perception sonore*, Ph.D. thesis, University of Aix-Marseille, 2021.

[22] K. F. Graff, *Wave Motion in Elastic Solids*, Dover Publications, New York, USA, 1991.

[23] Neville H Fletcher and Thomas D Rossing, *The physics of musical instruments*, Springer Science & Business Media, 2012.

[24] Stefan Bilbao, *Numerical sound synthesis: finite difference schemes and simulation in musical acoustics*, John Wiley & Sons, 2009.

[25] Mitsuko Aramaki, Mireille Besson, Richard Kronland-Martinet, and Sølvi Ystad, "Controlling the perceived material in an impact sound synthesizer," *IEEE Transactions on Audio, Speech, and Language Processing*, vol. 19, no. 2, pp. 301–314, 2010.

[26] Michele Ducceschi, Cyril Touzé, Olivier Thomas, and Stefan Bilbao, "Dynamics of the wave turbulence spectrum in vibrating plates: A numerical investigation using a conservative finite difference scheme," *Physica D*, vol. 280, pp. 73–85, 2014.

[27] Richard Kronland-Martinet, Sølvi Ystad, and Mitsuko Aramaki, "High-level control of sound synthesis for sonification processes," *AI & society*, vol. 27, no. 2, pp. 245–255, 2012.

[28] Samuel Poirot, Stefan Bilbao, Mitsuko Aramaki, and Richard Kronland-Martinet, "Sound morphologies due to non-linear interactions: Towards a perceptual control of environmental sound synthesis processes," in *DAFx2018*, 2018.